

SINUOSITY AS A MEASURE OF MIDDLE TROPOSPHERIC WAVINESS

by

Jonathan E. Martin¹, Stephen J. Vavrus², Fuyao Wang², and Jennifer A. Francis³

¹Department of Atmospheric and Oceanic Sciences, University of Wisconsin-Madison

²Center for Climatic Research, University of Wisconsin-Madison

³Institute of Marine and Coastal Sciences, Rutgers University

Submitted to *Climate Dynamics*: January 1, 2015

ABSTRACT

Despite the importance of synoptic- to planetary-scale atmospheric waves in the production of organized mid-latitude weather systems, no widely accepted metric exists for quantifying the waviness of the large-scale circulation. The concept of sinuosity, borrowed from geomorphology, is introduced as a means of measuring the waviness of the mid-tropospheric flow using 500 hPa geopotential height contours. A simple method for calculating the sinuosity of flow is presented and several broad characteristics of the flow are discussed.

First, the circulation is characterized by a maximum in waviness in the summer and a minimum in winter. Second, weakening (strengthening) of the mid-tropospheric zonal flow is shown to be associated with increased (decreased) waviness. Third, a strong negative correlation is found between the observed daily sinuosity and the daily Arctic Oscillation (AO) index in the cold season. Additionally, the DJF average sinuosity is shown to be highly correlated with the seasonal average AO index, suggesting that physical mechanisms that reduce (increase) the poleward height gradient, and correspondingly weaken (strengthen) the mid-latitude westerlies, may also encourage increased (reduced) waviness. The use of this metric to examine changes in the complexion of mid-latitude waviness in a changing climate is discussed as is calculation of the sinuosity using contours of potential vorticity (PV) at the tropopause.

1. Introduction

In recognition of the prominent role played by the mid-latitude westerlies in the general circulation of the Earth's atmosphere, Rossby and collaborators (1939) introduced the concept of the "zonal index"¹ as a measure of the strength of the zonal westerlies. Subsequent work by Namias (1950) examined what appeared to be a characteristic decline and recovery of the westerlies each winter in what he termed the "index cycle". This work represented the culmination of a series of investigations (e.g. Namias 1947a,b, Willett 1948, Wexler 1948) linking changes in the hemispheric circulation (evident in changes in the zonal index) to the equatorward movement of cold air during boreal winter. Central to this idea was the notion that strong, zonally oriented mid- to upper-tropospheric westerlies act to contain cold air at high latitudes so that cold-air outbreaks are afforded when the zonality of the flow relaxes.

The development of blocking ridges substantially interrupts the zonality of the flow and so has become a topic of considerable inquiry (e.g. Elliot and Smith 1949, Rex 1950ab, White and Clark 1975, Egger 1978, Austin 1980, Legenäs and Øakland 1983, Dole and Gordon 1983, Lupo and Smith 1995, Shabbar et al. 2001, Pelly and Hoskins 2003, Schwierz et al. 2004, Woollings et al. 2011, Masato et al. 2013, Barnes et al. 2014, Davini et al. 2014). Another feature at the center of studies of hemispheric circulation variability has been the circumpolar vortex (CPV) (e.g.

¹ Originally defined at sea-level as the average geostrophic wind in the latitude belt 35°N to 55°N. It is commonly evaluated aloft as well.

Markham 1985, Angell 1998, Davis and Benkovic 1992, Burnett 1993, Frauenfeld and Davis 2003, Rohli et al. 2005, Wrona and Rohli 2007). As noted by Frauenfeld and Davis (2003), assessment of variability in the size, strength and waviness of the circulation can all be considered in terms of measurable characteristics of the CPV.

To our knowledge, only two studies of the variability of the CPV have directly assessed the waviness of the mid-tropospheric flow. Rohli et al. (2005) borrowed a measure from fluvial geomorphology – the circularity ratio (R_c) – to quantify the waviness of the 5460m isohypse at 500 hPa (recommended by the study of Frauenfeld and Davis 2003) for the month of January from 1959-2001. Wrona and Rohli (2007) extended this analysis to DJF for each of those 43 cold seasons and added analyses of the months of April, July, and October in order to uncover aspects of the seasonality of the CPV, as depicted by this single 500 hPa isohypse.

High impact mid-latitude weather events and regimes are often associated with large-amplitude planetary waves, as such patterns are dynamically linked to robust cyclogenesis and anticyclogenesis events as well as the development of blocked flows. In spite of this well-known relationship, no widely accepted metric exists for quantifying the waviness of the circulation. Recent studies employing gridded reanalysis data sets have offered reasonable suggestions. Francis and Vavrus (2012) and Barnes (2013) have incorporated related, but distinct, measures of the maximum meridional extent of 500 hPa isohypses (on seasonal and daily time scales) as a means of examining interannual trends in the complexion of middle tropospheric waves. Screen and Simmonds (2013) employed a Fourier

decomposition to first characterize both the meridional and zonal amplitudes of waves in the mid-latitude middle troposphere, and then examine temporal changes in these characteristics. In the present paper we appropriate a measure common in geomorphology – *sinuosity* – to measure the waviness of the mid-tropospheric flow using 500 hPa geopotential height contours. As will be shown, calculation of this simple quantity ensures that any departure from zonality in geostrophic streamlines, *not only the most extreme departures*, is incorporated into a metric of hemispheric waviness. A seasonality in the sinuosity of the flow is demonstrated, with a maximum in summer and minimum in winter. Through consideration of a 500 hPa zonal index², a characteristic weakening of the mid-tropospheric zonal wind in association with an increase in sinuosity is demonstrated. Additionally, a strong negative correlation is found between the observed daily sinuosity and the daily Arctic Oscillation (AO) index in the cold season. Further, the winter (DJF) average sinuosity is shown to be highly correlated with the seasonal average AO, suggesting that the physical mechanisms that reduce (increase) the poleward height gradient and correspondingly weaken (strengthen) the mid-latitude westerlies, may also encourage increased (reduced) waviness.

The purpose of this paper is to introduce a new tool for assessing changes in the complexion of the large-scale circulation and to demonstrate fundamental aspects of its utility. Accordingly, the paper is organized in the following manner. In Section 2 we define sinuosity and describe both the method and data set used to

² The daily 500 hPa zonal index is calculated as the zonal average of the westerly geostrophic wind at 500 hPa in the latitude belt 35°-55°N.

calculate it. Aspects of the annual cycle in sinuosity, along with an emphasis on analysis of a time series of the previous 66 winter seasons, are presented in Section 3. The relationship between cold-season time series of sinuosity and the AO are also considered in that section. Finally, a summary and discussion of the results, including suggestions for future research, are offered in Section 4.

2. Data and Methodology

Morphological aspects of the meanders of rivers and streams is a subject in fluvial geomorphology. A simple measure of such meanders is known as sinuosity which is the ratio of the curvilinear length of a segment of a stream to the length of the shortest distance between the endpoints of the segment (Leopold et al. 1964). A schematic example is given in Fig. 1. The extension of this idea employed in the present study depends upon calculation of the curvilinear length of, and the area enclosed by, a given 500 hPa geopotential height contour (isohypse). Cutoff portions of any isohypse (i.e. cutoff lows or highs) are easily included in our measure of sinuosity since such features occupy a measurable area and their perimeters have finite curvilinear lengths. We consider the waviness in a given mid-latitude flow to be a measure of the departure of its streamlines from zonality. Therefore, determination of the sinuosity of the flow along a geostrophic streamline (i.e. isohypse) begins by calculating the area enclosed by the given isohypse. Next, we compute an equivalent latitude for that isohypse. The equivalent latitude is that latitude poleward of which the area is equal to the area enclosed by the given

isohypse³. Finally, the sinuosity is defined as the ratio of the curvilinear length of the given 500 hPa isohypse to the circumference of its equivalent latitude circle. An example is shown in Fig. 2. It follows from the definition that the minimum value of sinuosity is 1.0 which describes a purely zonal streamline (i.e. no waviness).

It has been suggested that shifting isohypses poleward in a warmer climate might give rise to the illusion, when using sinuosity as a metric, of a change in waviness when none is occurring. In order to evaluate this concern we conducted a series of simple numerical experiments in which the sinuosity of hypothetical isohypses, characterized by a varying number of deep and shallow square waves, were carefully examined. The simplest case of a single modest square wave is shown in Fig. 3. Keeping the aspect ratio of the square wave constant upon moving the isohypse from 35° to 40°N results in an 8.9° latitudinal depth at 40°N compared to the original 10° at 30°N. The poleward encroachment of this waveform results in a 0.24% increase in sinuosity at the higher latitude. We suggest this is well small enough to ensure that the utility of sinuosity as a metric of waviness is not compromised.

Though many prior investigations of the variability of the mid-tropospheric circulation have considered the area of the circumpolar vortex, only Rohli et al.

³ If A is the area enclosed by a given isohypse, then the equivalent latitude, ϕ_E , is given by $\phi_E = \arcsin[1 - \frac{A}{2\pi R_e^2}]$, where R_e is the radius of the Earth. Reference to an equivalent latitude is reminiscent of an aspect of the measure of eddy amplitude employed by Nakamura and Zhu (2010) and Nakamura and Solomon (2010, 2011) in their development of a diagnostic formulation for finite-amplitude wave activity.

(2005) and Wrona and Rohli (2007) explicitly considered the waviness. They did so using a measure called the circularity ratio (R_c) defined as the area enclosed within a given isohypse divided by the area poleward of a zonal ring whose perimeter is identically the curvilinear length of the given isohypse. They applied this measure to a single 500 hPa isohypse (546 dm) for 42 cold seasons (DJF) using observed mean monthly 500 hPa geopotential height analyses on a $5^\circ \times 5^\circ$ latitude/longitude grid from NCAR's Monthly Northern Hemisphere Tropospheric Analysis.⁴ Their choice of the 5460 m isohypse was motivated by the desire to consistently sample the size and shape of the circumpolar vortex within the main belt of the westerlies.

We employ the NCEP/NCAR reanalysis (NRA) data (Kalnay et al. 1996). Note that while direct comparisons of reanalysis values to observations is problematic owing to lack of independent measures, the upper-level circulation in the NRA has been found to be very similar to that of the reanalysis by the European Centre for Medium Range Weather Forecasts (Archer and Caldeira, 2008) and other reanalyses by Davini (2013). These data are available 4 times daily on a global $2.5^\circ \times 2.5^\circ$ grid and are derived from a frozen state-of-the-art global assimilation system in conjunction with a database that includes in-situ and remotely sensed data (when available) both at the surface and at levels through the troposphere and stratosphere. The present study calculates the sinuosity of a collection of individual 500 hPa isohypses in a domain covering 20°N to 90°N , using daily average 500 hPa heights constructed from the four times daily data, from 1 January 1948 to 28

⁴ These data are available at <http://dss.ucar.edu/datasets/ds085.1>

February 2014. In addition to calculating the sinuosity of individual 500 hPa isohypses, we also calculate the aggregate sinuosity of a set of 5 isohypses (576, 564, 552, 540, and 528 dm) which contain the maximum 500 hPa geostrophic wind throughout the year. The aggregate sinuosity at a given time is simply the ratio of the sum of the lengths of all 5 isohypses to the sum of the circumferences of the 5 equivalent latitude circles at that time⁵.

A note regarding the differences between circularity ratio and sinuosity as separate measures of the waviness is warranted. Calculation of circularity ratio for a given isohypse requires determination of a latitude, ϕ_p , at which the length of a zonal streamline is equal to the curvilinear length of the isohypse. Since the *areal extent*, not the length, of a given isohypse is directly related to a first order atmospheric variable (i.e. average temperature in the underlying troposphere via the hypsometric relationship), we suggest that sinuosity is a more physically relevant measure of the waviness. Furthermore, the present analysis, in contrast to those by Rohli et al. (2005) and Wrona and Rohli (2007), considers an annual cycle in waviness, relates the waviness metric to an important mode of large-scale atmospheric variability (the Arctic Oscillation), and incorporates a range of isohypses to more comprehensively characterize the complexion of middle

⁵ One can choose any set of consecutive isohypses to produce an aggregate sinuosity. The choice made here is motivated by a desire to sample in the main belt of the westerlies. The aggregate sinuosity here is given by

$$S_5 = \frac{[L_{576} + L_{564} + L_{552} + L_{540} + L_{528}]}{[EL_{576} + EL_{564} + EL_{552} + EL_{540} + EL_{528}]}$$

where L is the length of the indicated isohypse and EL is the length of its corresponding equivalent latitude circle.

tropospheric waves across a broader extratropical domain. The mathematical relationship between the two measures is presented in the Appendix.

3. Results

In order to examine the waviness of the 500 hPa flow in as comprehensive a manner as possible, the following analysis is split into two broad categories. We first consider the results of the 5 contour aggregate sinuosity calculations and then move to evaluation of the characteristics of individual isohypses.

a. Aggregate sinuosity

The 500 hPa aggregate sinuosity analysis presented here considers the 576, 564, 552, 540, and 528 dm geopotential height contours and will be referred to as S_5^6 . Each of these contours encloses a certain amount of area. Equal area is contained poleward of an equivalent latitude (ϕ_{EQ}) and the length of the zonal ring at ϕ_{EQ} represents the shortest possible perimeter that can enclose the given amount of area. The contour length of a given isohypse is determined by summing its segments in each $2.5^\circ \times 2.5^\circ$ grid box calculated using the Spherical Law of Cosines formula;

$$L = a \cos[\sin \phi_1 \sin \phi_2 + \cos \phi_1 \cos \phi_2 \cos(\lambda_2 - \lambda_1)] R_e$$

⁶ The correlation of the seasonal (DJF) average zonal index with seasonal average S_5 is -0.651.

where (ϕ_1, λ_1) and (ϕ_2, λ_2) represent the latitude and longitude coordinates where the given isohypse intersects the boundaries of a grid box and R_e is the radius of the Earth.

The analysis presented here focuses on the winter (DJF) as it is during this season that the mid-latitude flow is at its energetic peak and the Arctic Oscillation exerts its strongest influence on the large-scale. The 66-year time series of DJF-average aggregate sinuosity is shown in Fig. 4. Over the course of this time series, a slight, and statistically insignificant, upward trend in the aggregate sinuosity appears. Since ~1990, however, a more rapid increase in aggregate sinuosity appears to be emerging.

The pronounced wintertime increase in sinuosity during the past two decades, and the exceptionally high values in 2009-10 and 2010-11, suggests a possible relationship with the Arctic Oscillation (AO), which reached its strongest positive phase during the winter of 1989-1990 and strongest negative phase in winter 2009-10. Because mid-latitude circulation during the positive (negative) phase of the AO tends to be anomalously zonal (wavy), sinuosity should be able to capture this behavior quantitatively. Employing the daily Arctic Oscillation (AO) time series from 1 December 1950 to present, the correlation between the daily aggregate sinuosity of the 500 hPa flow and the AO index for each DJF season since 1950-51 is shown in Fig. 5. Twenty-three of 64 years exhibit a very strong relationship ($r \leq -0.6$) between the AO index and our measure of sinuosity. In 43 of the 64 years $r \leq -0.4$, indicating a strong relationship between the two time series.

Additional insight into this relationship arises from consideration of the seasonal average AO index compared to the seasonal average sinuosity, as shown in Fig. 6. It is clear that enhanced waviness in the 500 hPa flow is associated with a negative AO.

b. Annual cycle of sinuosity

The annual cycle of waviness is another aspect of the large-scale behavior of the mid-latitude atmosphere that can be interrogated using sinuosity. An annual cycle of the aggregate sinuosity was constructed by taking each calendar day's average sinuosity over the 66-year time series. The results of this analysis are shown in Fig. 7. Immediately apparent is the fact that the aggregate sinuosity reaches its maximum in the summer and its minimum in the winter. In fact, there is a broad peak in waviness that characterizes the warm season (April to October) with peak values of S_5 near 1.9 in early July and a fairly flat period of minimum values (~ 1.45) occurring in DJF. Also of note is the near symmetry of sinuosity on either side of the peak value as well as the fact that the peak in S_5 slightly precedes the minimum in mean areal extent of lower tropospheric cold air (\sim July 12-15) as reported by Martin (2015). Finally, the annual cycle of 500 hPa zonal index is overlaid with the daily average S_5 in Fig. 7 indicating the nearly perfect inverse relationship between these two time series (they are correlated at $r = -0.9506$).

The annual cycle of sinuosity for the 5 individual isohypses that compose the aggregate are shown, along with the aggregate, in Fig. 8. There is a clear dichotomous structure exhibited amongst these 5 time series. The 576 dm isohypse (red) exhibits the smallest annual cycle in waviness with evidence of two separate

peaks, the most prominent one near August 1 and a secondary peak near mid-October. The 564 dm isohypse (orange) is characterized by the sharpest peak (maximizing in early July) but the tails of its annual cycle are not symmetric. The sinuosity is much lower (near 1.3) from January ~15 March whereas it persists well above 1.3 from mid-October to the end of December. A broad warm-season peak also characterizes the 552 dm isohypse (blue) though it reaches its peak value in mid-June. The warm season increase in sinuosity of this streamline also demonstrates a double peak with the secondary maximum centered around August 1.

It must be noted that the calculation of daily average sinuosity for individual isohypses includes only those days on which a value exists. This method ensures that whenever the contour does not exist on a given day, its absence does not dilute the average value of sinuosity for the calendar day. This is an important qualification when considering the dramatically different annual cycles exhibited by the 540 (green) and 528 dm (magenta) isohypses (Fig. 8). The areal extent of both of these values of geopotential height shrinks dramatically in the warm season. In fact, for a number of calendar days in late July, more than half of all years had a lower troposphere warm enough to preclude the existence of the 528 dm isohypse. The fact that this is not the case for the 540 dm isohypse⁷, and yet it displays a

⁷ July 25 is the calendar day with the highest number (3) of missing 540 dm isohypses. In the entire 66-year time series, there are a total of only 28 such days for 540 dm whereas there are 1934 such days for 528 dm.

similar annual cycle of sinuosity, suggests that there is truly a minimum in waviness at high latitudes during the warm season.

The annual cycle of sinuosity of the 528 dm isohypse, along with an indication of the portions of the year when the 528 dm is frequently absent, is shown in Fig. 9. From July 15-27⁸, more than 50% of the time series did not contain a 528 dm isohypse. Interestingly, the spring (autumn) peak in sinuosity occurs before (after) the first calendar day on which the 528 dm streamline is nonexistent. This fact suggests that the similar dual spring/autumn sinuosity maxima exhibited by the nearly omnipresent 540 dm isohypse reflects a real variation in high latitude waviness over the course of the year.

c. Relation of the annual cycle in S_5 to morphological features of the NH circulation

Cut-off lows (COLs) are closed cyclonic circulations in the upper troposphere that have become detached from, and often subsequently migrate equatorward of, the main westerlies (Gimeno et al. 2007). As described previously, our calculation of sinuosity takes explicit account of the contributions from COLs as well as cutoff anticyclones. Such features invariably increase the sinuosity of a given geopotential height contour and so contribute to increases in S_5 as well.

The seasonal cycle of aggregate sinuosity is consistent with the higher incidence of mid-tropospheric COLs that characterizes the Northern Hemisphere

⁸ July 17 and 21 are slight exceptions to this category, missing only 29 and 32 representatives in the 66-year time series.

warm season (Parker et al. 1989, Bell and Bosart 1989, Wernli and Sprenger 2007, Nieto et al. 2008). In fact, Nieto et al. (2008) found that 41% of all COLs identified in the NCEP Reanalysis data from 1948-2006 occurred in JJA while only 17% occurred in DJF. Additionally they found that the frequency of autumn (SON) COLs slightly exceeds that of spring (see their Fig. 14). This is consistent with the secondary peak in S_5 that appears in September/October in the present analysis (see Fig. 6).

Parker et al. (1989) also considered the distribution of 500 hPa closed anticyclones (blocking highs) in their 36 year climatology. Such features are substantially less frequent than COLS. Though anticyclones needn't be closed to have a substantial impact on sinuosity (e.g. high amplitude, open ridges greatly increase S_5), they found that these disturbances are most frequent over the subtropics with highest incidence in the warm season.

The coincidence of these various synoptic-climatological features suggests the following explanation for the seasonal cycle in sinuosity. As the minimally wavy wintertime circumpolar vortex shrinks with the coming spring, cutoff lobes of low geopotential height are orphaned at low latitudes where increasingly intense insolation quickly relaxes their associated tropospheric cold anomalies and corresponding negative 500 hPa height anomalies. The warm season maximum in COLs and blocking highs accounts for the summertime maximum in S_5 . The late summer/early autumn presence of tropical cyclones, and their inevitable recurvature to middle-latitudes, provides a seasonally unique mechanism for the growth of mid-latitude ridges in that season that accounts for the secondary

autumnal peak in sinuosity previously noted. Finally, it is hypothesized that the decline of sinuosity in the autumn transition to winter is a function of the absorption of cutoffs that results from the expansion of the circumpolar vortex as the hemisphere cools.

4. Discussion and Conclusions

Despite the fact that a substantial fraction of high impact mid-latitude weather events and regimes are associated with large-amplitude planetary waves, no widely accepted metric exists for quantifying the waviness of the circulation. In this paper we have introduced the concept of sinuosity as a new tool for measuring waviness and applied it to a set of 500 hPa geopotential height contours that contain the maximum wind throughout the year.

A seasonality in the sinuosity of the flow has been demonstrated, with a maximum in summer and minimum in winter. It has also been demonstrated that a weakening of the mid-tropospheric zonal wind is closely associated with an increase in sinuosity. Additionally, a strong negative correlation exists between the observed daily sinuosity and the daily Arctic Oscillation (AO) index in the cold season. Further, the winter (DJF) average sinuosity is shown to be highly correlated with the seasonal average AO, suggesting that the physical mechanisms that reduce (increase) the poleward height gradient and correspondingly weaken (strengthen) the mid-latitude westerlies, may also encourage increased (reduced) waviness.

We have calculated sinuosity based on 500 hPa height contours in this paper as a means of characterizing the waviness of the broad middle tropospheric flow.

An extension of the method outlined here, that would more specifically assess the waviness of the tropopause-level jet stream, would be to calculate the sinuosity of contours of constant potential vorticity (PV) (referred to as *isertels* by Morgan and Nielsen-Gammon 1998). Since the tropopause-level jet is coincident with strong gradients in PV and is found on the low PV edge of such a gradient, calculation of the sinuosity of, for instance, the 2 PVU isertel would render a clear picture of the waviness of the tropopause-level jet stream itself. Complicating matters is the fact that two distinct species of tropopause-level jets, the polar and subtropical jet, are present nearly all the time. Isolation of one from the other can be accomplished through consideration of the isertels in separate isentropic layers that contain the separate jets. We plan to pursue this issue in future work.

Recent studies by Francis and Vavrus (2012) and Barnes (2013) have examined the question of whether Arctic amplification has caused planetary-scale waves to become wavier and less progressive resulting in more frequent blocking and associated severe weather. The question remains an open one at present. We feel that continued refinement of our sinuosity metric promises to enlighten that debate as well as other questions regarding the complexion of the middle-tropospheric flow in a changing climate. To that end, we are currently exploring the nature of the response in sinuosity to a variety of climate change scenarios using output from the CMIP-5 suite of models.

REFERENCES

- Angell, J. K., 1998: Contraction of the 300 mbar north circumpolar vortex during 1963-1997 and its movement into the Eastern Hemisphere. *J. Geophys. Res.*, **103**, 25887-25893.
- Austin, J. F., 1980: The blocking of middle latitude westerly winds by planetary waves. *Quart. J. Roy. Meteor. Soc.*, **106**, 327-350.
- Archer, C. L., and K. Caldeira, 2008: Historical trends in the jet streams. *Geophys. Res. Lett.*, **35**, L08803, doi:10.1029/2008GL033614.
- Barnes, E. A., E. Dunn-Sigouin, G. Masato, and T. Woollings, 2014: Exploring recent trends in Northern Hemisphere blocking. *Geophys. Res. Lett.*, **41**, doi:10.1002/2013GL058745.
- Barnes, E. A., 2013: Revisiting the evidence linking Arctic amplification to extreme weather in midlatitudes. *Geophys. Res. Lett.*, **40**, 1-6, doi:10/1002/GRL.50880.
- Bell, G. D., and L. F. Bosart, 1989: A 15-year climatology of Northern Hemisphere 500 mb closed cyclone and anticyclone centers. *Mon. Wea. Rev.*, **117**, 2141-2163.
- Burnett, A. W., 1993: Size variations and long-wave circulation within the January Northern Hemisphere circumpolar vortex: 1946-89. *J. Climate*, **6**, 1914-1920.

- Davini, P., C. Cagnazzo, and J. A. Anstey, 2014: A blocking view of the stratosphere-troposphere coupling. *J. Geophys. Res.*, **119(19)**, 11100-11115.
- Davini, T. D., 2013: Atmospheric blocking and mid-latitude climate variability. Ph. D. dissertation, *Programme in Science and Management of Climate Change*, University of Foscari, Italy.
- Davis, R. E., and S. R. Benkovic, 1992: Climatological variations in the Northern Hemisphere circumpolar vortex in January. *Theoretical and Applied Climatology*, **46**, 63-73.
- Dole, R. M., and N. D. Gordon, 1983: Persistent anomalies of the extratropical Northern Hemisphere wintertime circulation: Geographical distribution and regional persistence characteristics. *Mon. Wea. Rev.*, **111**, 1567-1586.
- Egger, J., 1978: Dynamics of blocking highs. *J. Atmos. Sci.*, **35**, 1788-1801.
- Elliot, R. D., and T. B. Smith, 1949: A study of the effect of large blocking highs on the general circulation in the northern hemisphere westerlies. *J. Meteor.*, **6**, 67-85.
- Francis, J. A., and S. J. Vavrus, 2012: Evidence linking Arctic amplification to extreme weather in mid-latitudes. *Geophys. Res. Lett.*, **39(6)**, L06801, doi:10.1029/2012GL051000.
- Frauenfeld, O. W., and R. E. Davis, 2003: Northern Hemisphere circumpolar vortex trends and climate change implications. *J. Geophys. Res.*, **108**, 4423- doi:10.1029/2002/JD002958.

- Gimeno, L., R. M. Triego, P. Ribera, and J. A. Garcia, 2007: Editorial: Special issue on cut-off low systems (COL). *Meteorol. Atmos. Phys.*, **96**, 1-2, doi:10.1007/s00703-006-0216-5.
- Kalnay, E. et al., 1996: The NCEP/NCAR 40-year reanalysis project. *Bull. Amer. Meteor. Soc.*, **77**, 437-471.
- Lejenäs, H., and H. Øakland, 1983: Characteristics of northern hemisphere blocking as determined from long time series of observational data. *Tellus*, **35A**, 350-362.
- Lupo, A. R., and P. J. Smith, 1995: Climatological features of blocking anticyclones in the Northern Hemisphere. *Tellus*, **47A**, 439-456.
- Markham, C. G., 1985: A quick and direct method for estimating mean monthly global temperatures from 500 mb data. *Professional Geographer*, **37**, 72-74.
- Martin, J. E., 2015: Contraction of the Northern Hemisphere, lower tropospheric, wintertime cold pool over the last 66 years. *J. Climate*, **28**, (submitted).
- Masato, G., B. J. Hoskins, and T. J. Woollings, 2013: Winter and summer Northern Hemisphere blocking in CMIP5 models. *J. Climate*, **26**, 7044-7059.
- Morgan, M. C., and J. W. Nielsen-Gammon, 1998: Using tropopause maps to diagnose midlatitude weather systems. *Mon. Wea. Rev.*, **126**, 2555-2579.

Nakamura, N. and D. Zhu, 2010: Finite-amplitude wave activity and diffusive flux of potential vorticity in eddy-mean flow interaction. *J. Atmos. Sci.*, **67**, 2701-2716.

____, and A. Solomon, 2010: Finite-amplitude wave activity and mean flow adjustments in the atmospheric general circulation. Part I: Quasigeostrophic theory and analysis. *J. Atmos. Sci.*, **67**, 3967-3983.

____, and _____, 2011: Finite-amplitude wave activity and mean flow adjustments in the atmospheric general circulation. Part II: Analysis in the isentropic coordinate. *J. Atmos. Sci.*, **68**, 2783-2799.

Namias, J., 1950: The index cycle and its role in the general circulation. *J. Meteor.*, **7**, 130-139.

Namias, J., 1947a: Physical nature of some fluctuations in the speed of the zonal circulation. *J. Meteor.*, **4**, 125-133.

Namias, J., 1947b: Characteristics of the general circulation over the northern hemisphere during the abnormal winter of 1946-47. *Mon. Wea. Rev.*, **75**, 145-152.

Nieto, R., M. Sprenger, H. Wernli, R. M. Triego, and L. Gimeno, 2008: Identification and climatology of cut-off lows near the tropopause. *Trends and Directions in Climate Research: Ann. N. Y. Acad. Sci.* 1146: 256-290, doi:10.1196/annals.1446.016.

- Parker, S. S., J. T. Hawes, S. J. Colucci, and B. P. Hayden, 1989: Climatology of 500 mb cyclones and anticyclones, 1950-85. *Mon. Wea. Rev.*, **117**, 558-570.
- Pelly, J., and B. J. Hoskins, 2003: A new perspective on blocking. *J. Atmos. Sci.*, **60**, 743-755.
- Rex, D. F., 1950a: Blocking action in the middle troposphere and its effect upon regional climate. Part I: An aerological study of blocking action. *Tellus*, **2**, 196-211.
- Rex, D. F., 1950b: Blocking action in the middle troposphere and its effect upon regional climate. Part II: The climatology of blocking action. *Tellus*, **2**, 275-301.
- Rohli, R. V., K. M. Wrona, and M. J. McHugh, 2005: January northern hemisphere circumpolar vortex variability and its relationship with hemispheric temperature and regional teleconnections. *Int. J. Climatol.*, **25**, 1421-1436.
- Rossby, C.-G., and collaborators, 1939: Relations between variations in the intensity of the zonal circulation of the atmosphere and the displacements of the semi-permanent centers of action. *J. Marine Res.*, **2**, 38-54.
- Schwierz, C., M. Croci-Maspoli, and H. C. Davies, 2004: Perspicacious indicators of atmospheric blocking. *Geophys. Res. Lett.*, **31**, L06125, doi:10.1029/2003GL019341.

- Screen, J. A., and I. Simmonds, 2013: Exploring links between Arctic amplification and mid-latitude weather. *Geophys. Res. Lett.*, **40**, 1-6, doi:10.1002/GRL.50174.
- Shabbar, A., J. Huang, and K. Higuchi, 2001: The relationship between the wintertime North Atlantic Oscillation and blocking episodes in the North Atlantic. *Int. J. Climatol.*, **21**, 355-369.
- Wernli, H., and M. Sprenger, 2007: Identification and ERA-15 climatology of potential vorticity streamers and cutoffs near the extratropical tropopause. *J. Atmos. Sci.*, **64**, 1569-1586.
- Wexler, H., 1948: A note on the record low temperature in the Yukon Territory January-February 1947. *Bull. Amer. Meteor. Soc.*, **29**, 547-550.
- White, W. B., and N. E. Clark, 1975: On the development of blocking ridge activity over the central North Pacific. *J. Atmos. Sci.*, **32**, 489-502.
- Willett, H. C., 1948: Patterns of world weather changes. *Trans. Amer. Geophys. Union*, **29**, 803-809.
- Woollings, T., J. G. Pinto, and J. A. Santos, 2011: Dynamical evolution of north Atlantic ridges and poleward jet stream displacements. *J. Atmos. Sci.*, **68**, 954-963.
- Wrona, K. M., and R. V. Rohli, 2007: Seasonality of the northern hemisphere circumpolar vortex. *Int. J. Climatol.*, **27**, 697-713.

FIGURE CAPTIONS

Fig. 1 Schematic illustrating the concept of sinuosity. S_{AB} is the ratio of the length of the blue contour to the length of the red line segment AB.

Fig. 2 Blue line is the daily average 552 dm geopotential height contour at 500 hPa on 18 January 2014. The area enclosed by that line is equal to the area enclosed by the red circle (the equivalent latitude). S_{552} is equal to the ratio of the length of the blue line to the length of the red line (1.2719).

Fig. 3 Schematic illustration of the negligible effect that poleward migration of isohypses has on sinuosity of a given contour. Original contour (in red) is zonal at 35N with a square wave of latitudinal depth 10. Displace contour (in blue) is zonal at 40N with square wave whose aspect ratio (longitudinal extent/latitudinal extent) is identical to original wave. The displaced contour has sinuosity 1.0024 times that of original contour.

Fig. 4 Time series of DJF season averaged, aggregate sinuosity from 1948-49 to 2013-14.

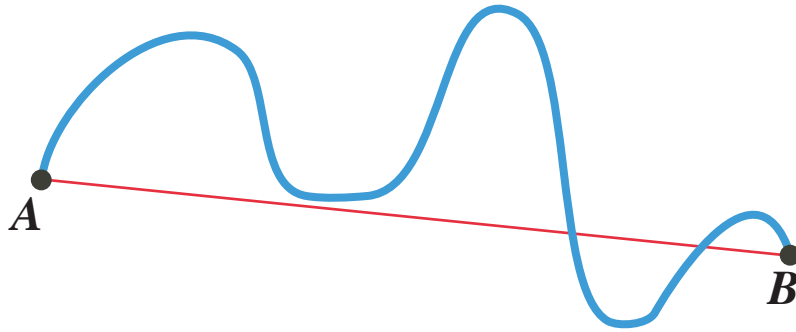
Fig. 5 Time series of correlation coefficient, r , between the daily AO index and the daily value of 500 hPa sinuosity (S_5) from 1950-51 to 2013-14. Green (blue) dots represent seasons with $r < -0.4$ (-0.6).

Fig. 6 Time series of DJF seasonal averaged AO index (red) compared to DJF seasonal averaged sinuosity (S_5) (blue). The two time series are correlated with $r = -0.520$, significant above the 99% level.

Fig. 7 Daily average aggregate sinuosity (solid black line) derived from 66-year NCEP Reanalysis time series. Gray shaded region represents $\pm 1\sigma$ around the daily mean. Daily average 500 hPa zonal index (ZI in m s^{-1} , blue solid line) derived from the same data set.

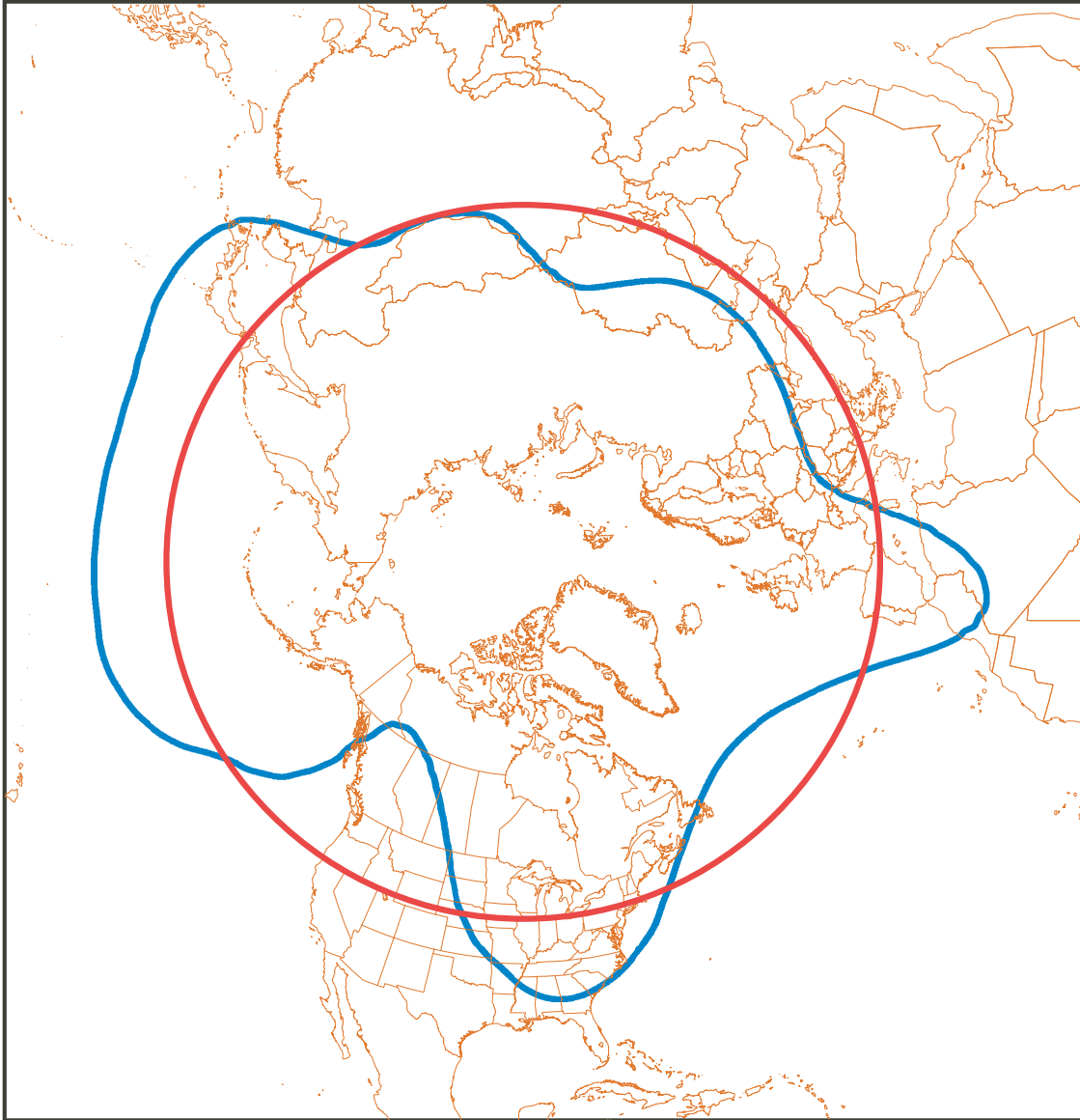
Fig. 8 Solid black line is the daily average aggregate sinuosity derived from 66-year NCEP Reanalysis time series. Daily average sinuosity of individual geopotential height contours in the set of 5 used in the aggregate calculation are indicated by the labeled colored lines.

Fig. 9 Annual cycle of the 528 dm isohypse (purple line) as compared to the annual cycle of the 5 contour aggregate sinuosity (solid black line). Gray shading indicates the range of calendar days on which the 528 dm isohypse is absent over the Northern Hemisphere. There are no missing days in regions without shading, at least one but not more than 10% in the lightest shading, 10-25% missing in the next darker shading, 25-590% in the next darker shade, and more than 50% missing in the darkest shading.



$$S_{AB} = \frac{(\text{Length of CONTOUR})}{(\text{Length of SEGMENT})}$$

Fig. 1 Schematic illustrating the concept of sinuosity. S_{AB} is the ratio of the length of the blue contour to the length of the red line segment AB.



500 hPa Z 18 January 2014

Fig. 2 Blue line is the daily average 552 dm geopotential height contour at 500 hPa on 18 January 2014. The area enclosed by that line is equal to the area enclosed by the red circle (the equivalent latitude). S_{552} is equal to the ratio of the length of the blue line to the length of the red line (1.2719).

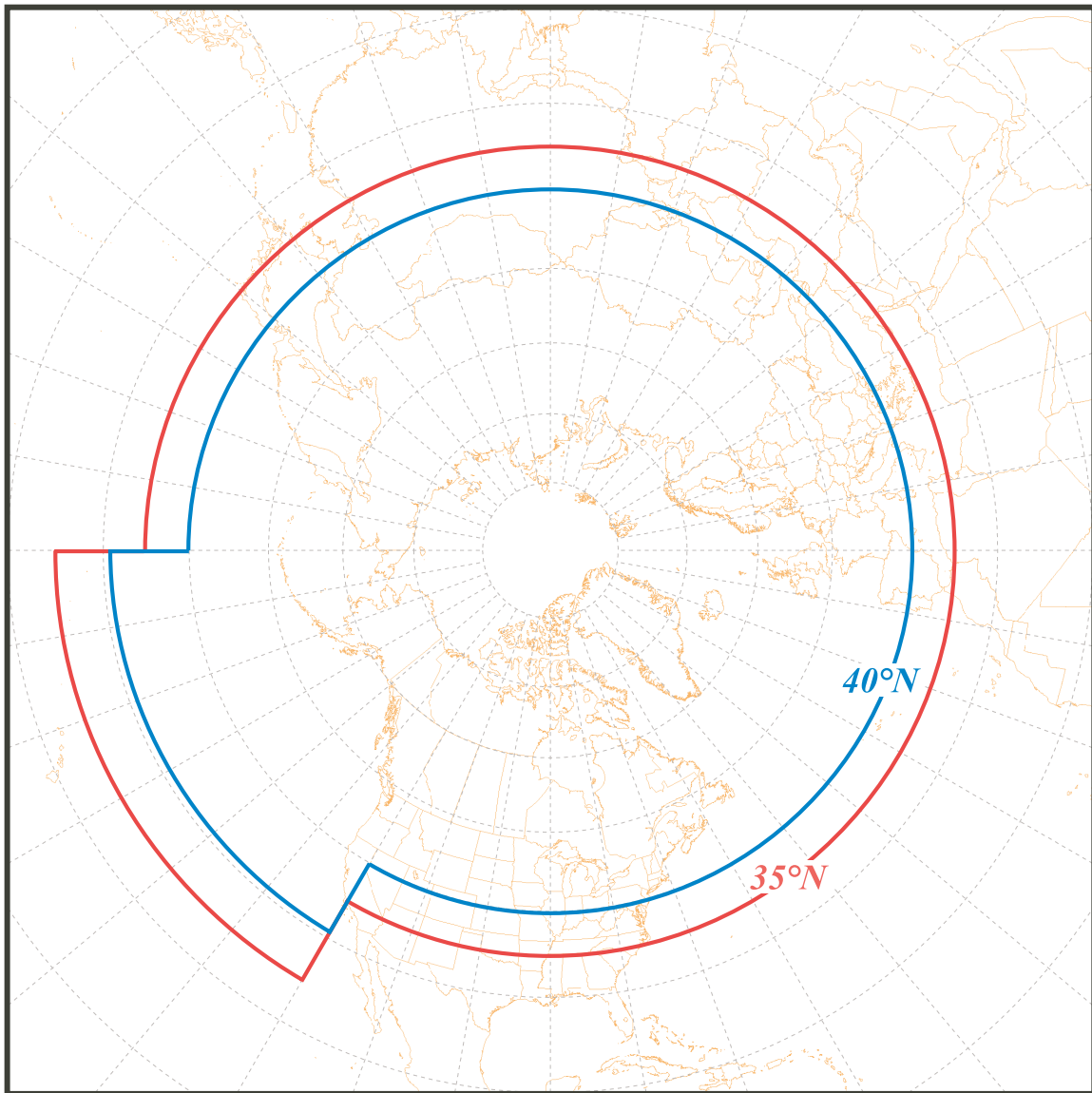


Fig. 3 Schematic illustration of the negligible effect that poleward migration of isohypses has on sinuosity of a given contour. Original contour (in red) is zonal at 35°N with a square wave of latitudinal depth 10°. Displaced contour (in blue) is zonal at 40°N with square wave whose aspect ratio (longitudinal extent/latitudinal extent) is identical to original wave. The displaced contour has sinuosity 1.0024 times that of original contour.

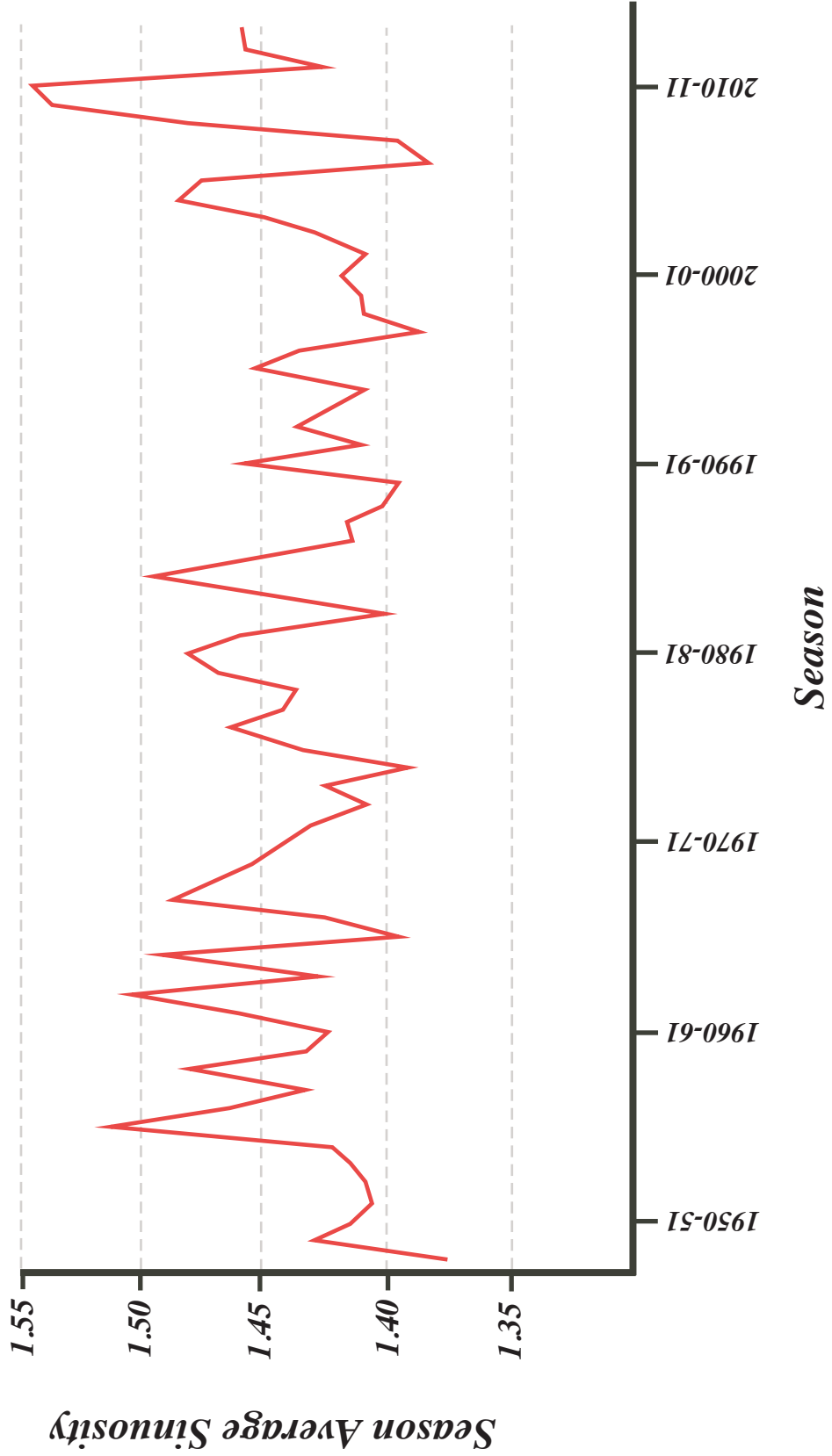


Fig. 4 Time series of DJF season averaged, aggregate sinuosity from 1948-49 to 2013-14.

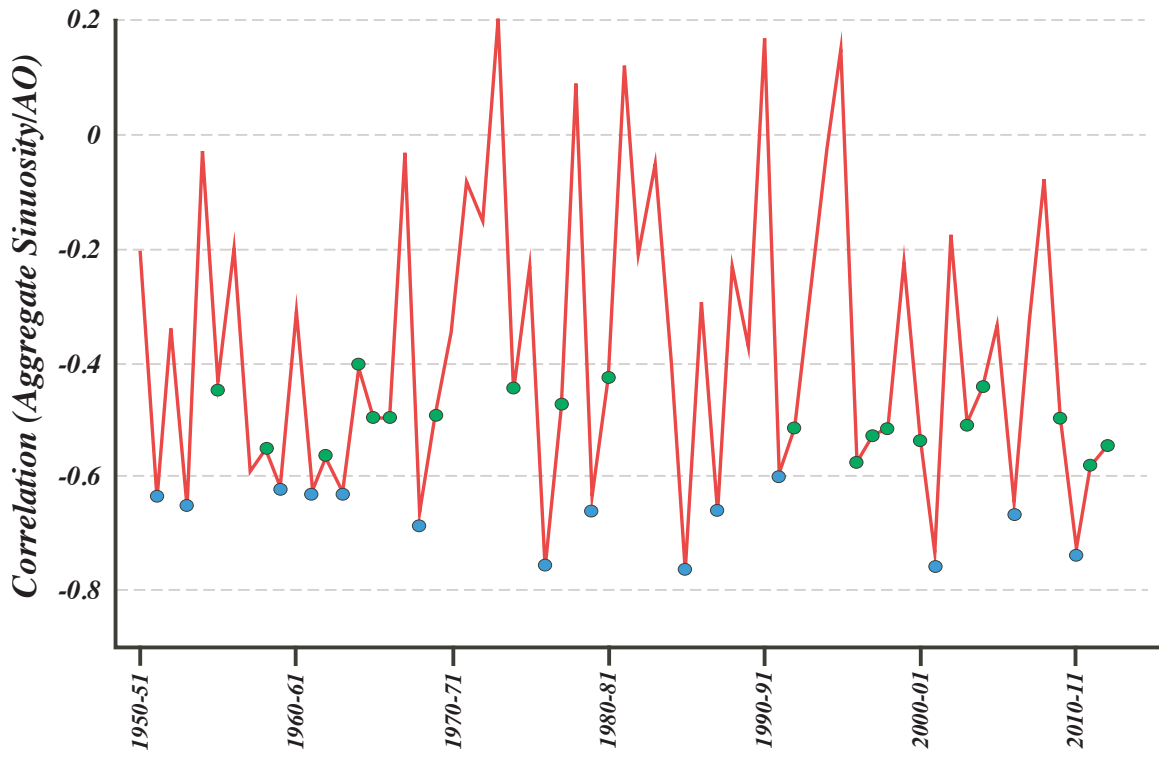


Fig. 5 Time series of correlation coefficient, r , between the daily AO index and the daily value of 500 hPa sinuosity from 1950-51 to 2013-14. Green (blue) dots represent seasons with $r < -0.4$ (-0.6).

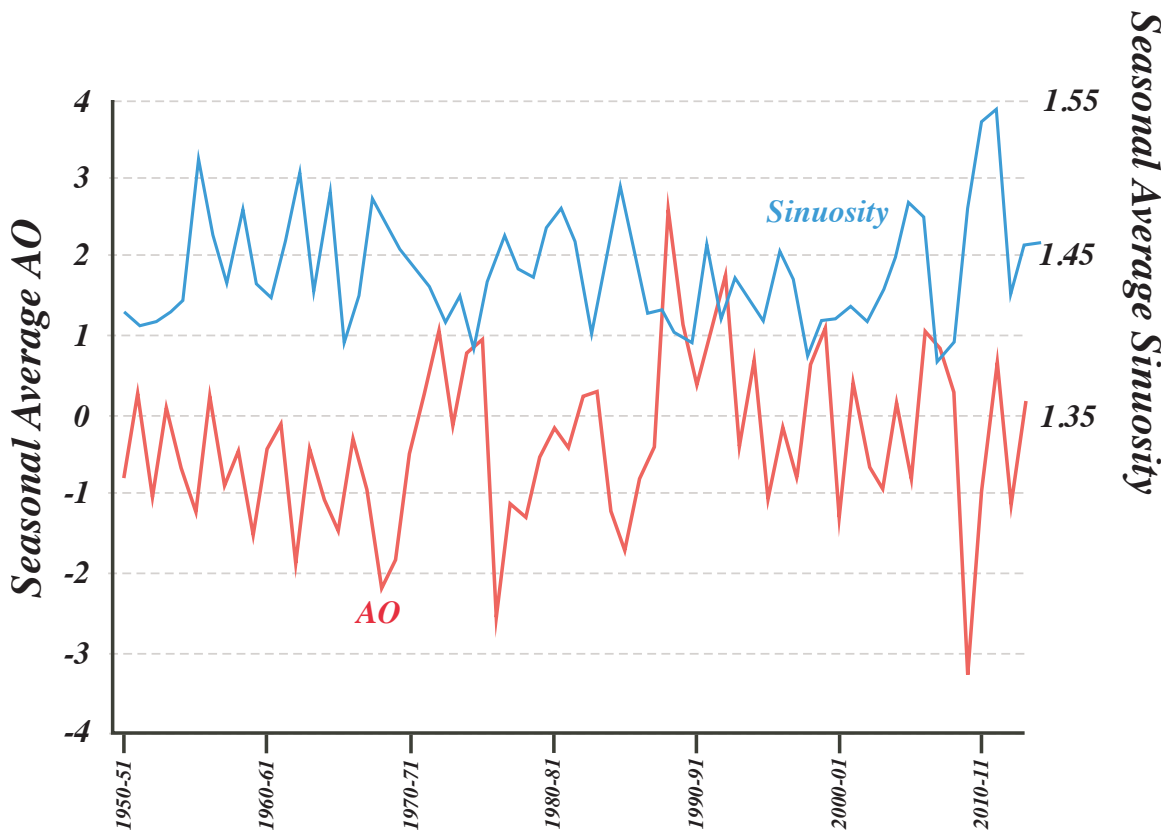


Fig. 6 Time series of DJF seasonal averaged AO index (red) compared to the DJF seasonal averaged sinuosity (blue). The two time series are correlated with $r = -0.520$, significant above the 99% level.

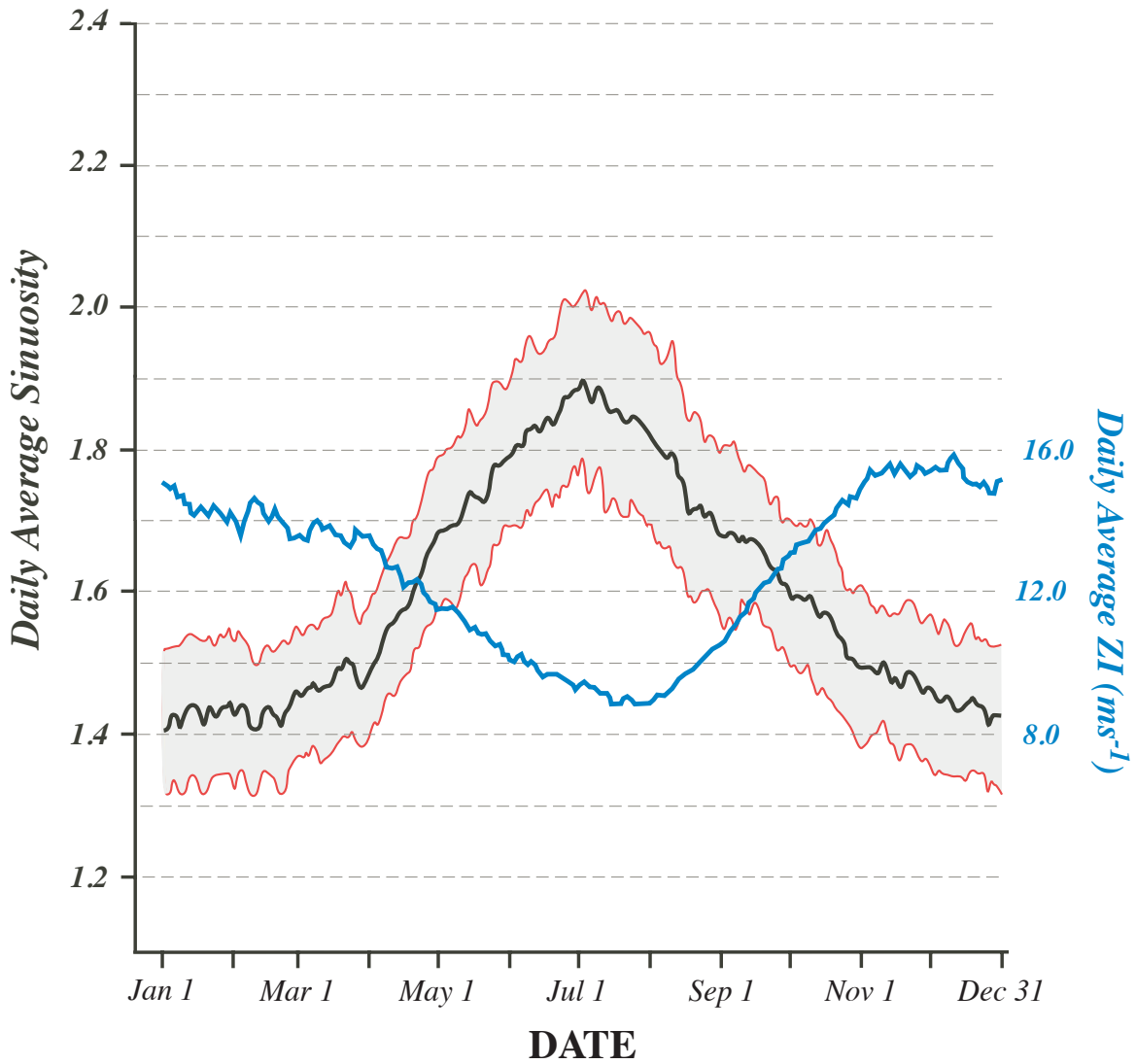


Fig. 7 Daily average aggregate sinuosity (solid black line) derived from 66-year NCEP Reanalysis time series. Gray shaded region represents $\pm 1\sigma$ around the daily mean. Daily average 500 hPa zonal index (ZI in ms^{-1} , blue solid line) derived from the same data set.

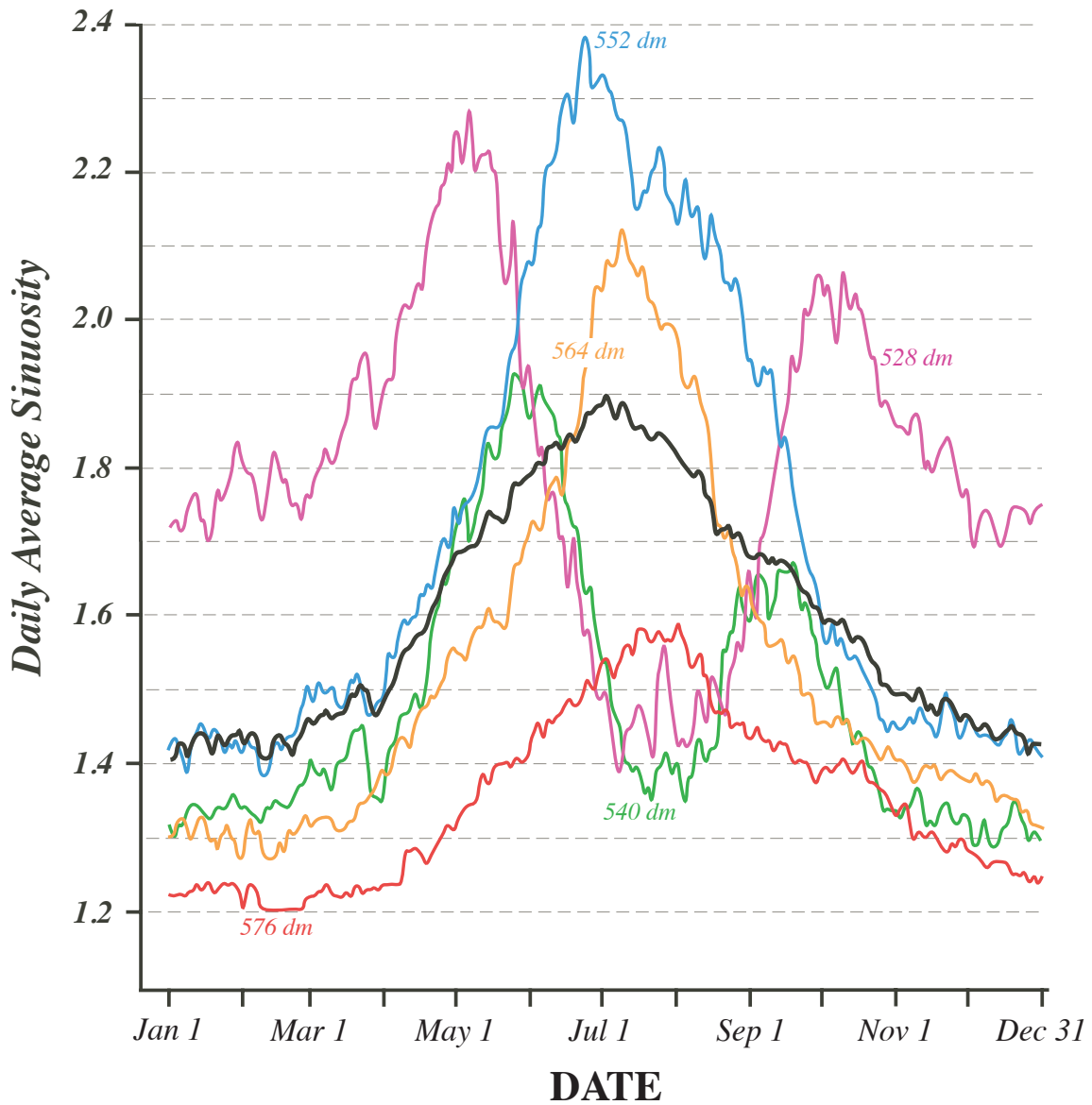


Fig. 8 Solid black line is the daily average aggregate sinuosity derived from 66-year NCEP Reanalysis time series. Daily average sinuosity of individual geopotential height contours in the set of 5 used in the aggregate calculation are indicated by the labeled colored lines.

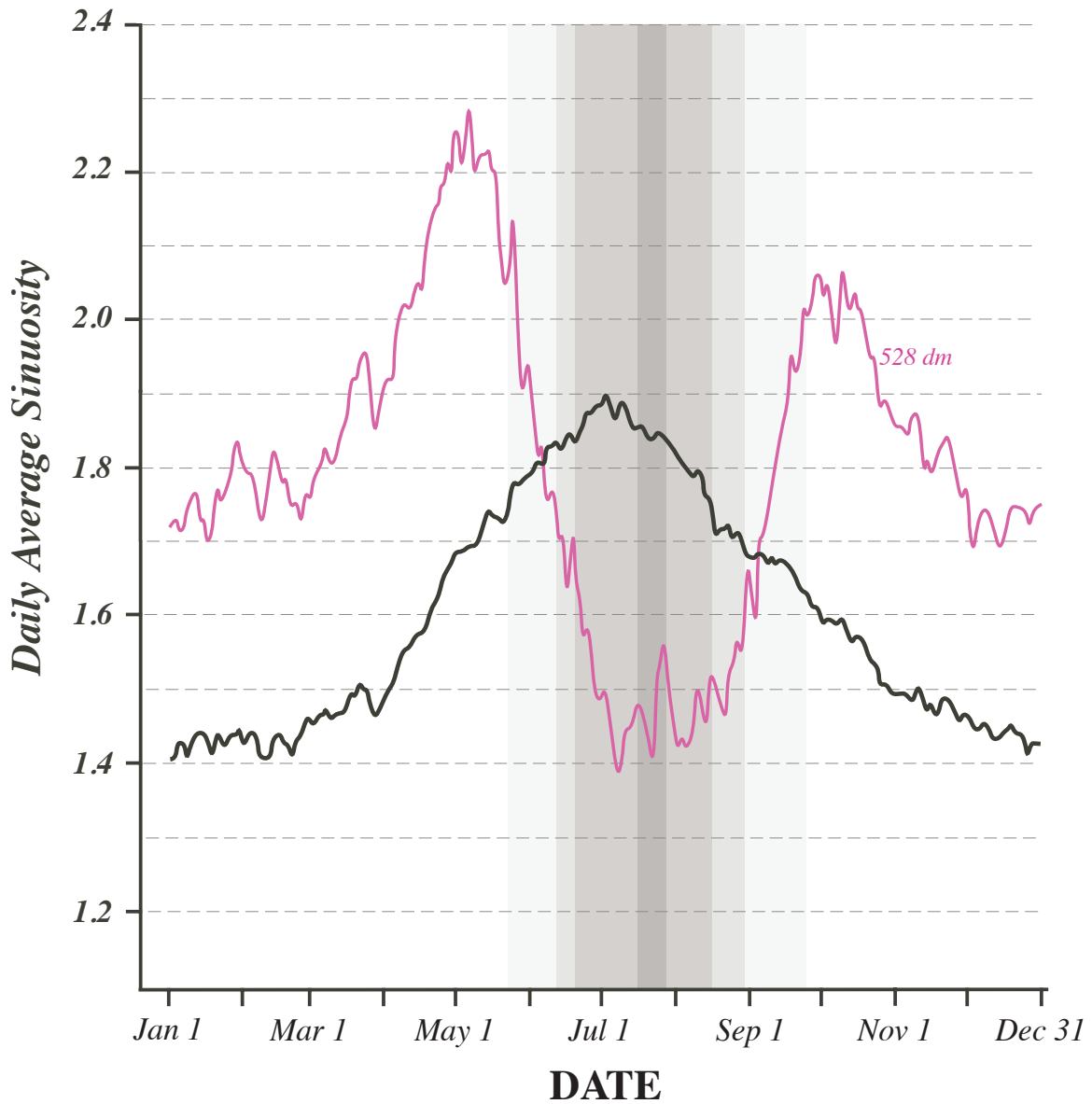


Fig. 9 Annual cycle of the 528 dm isohypse (purple line) as compared to the annual cycle of the 5 contour aggregate sinuosity (solid black line). Gray shading indicates the range of calendar days on which the 528 dm isohypse is absent over the Northern Hemisphere. There are no missing days in regions without shading, at least one but not more than 10% in the lightest shading, 10 - 25% missing in next darker shading, 25-50% in the next darker shade, and more than 50% missing in the darkest shading.